Nuclear Materials and Energy 000 (2017) 1–6

Contents lists available at ScienceDirect

Nuclear Materials and Energy

journal homepage: www.elsevier.com/locate/nme

Optimization of pumping efficiency and divertor operation in DEMO

S. Varoutis*, F. Bonelli, Chr. Day, Yu Igitkhanov

Karlsruhe Institute of Technology (KIT), Institute of Technical Physics, Vacuum Department, Karlsruhe, Germany

ARTICLE INFO

Article history:
Received 8 July 2016
Revised 22 February 2017
Accepted 1 April 2017
Available online xxx

Keywords:
DEMO
Divertor
Fueling
Pumping efficiency
DSMC method

ABSTRACT

In the present work a sensitivity analysis of the pumping performance of a standard divertor design for two extreme dome cases (with and without) and different pumping port locations is performed. Such an investigation re-assesses the role of the divertor dome in the design of a DEMO divertor cassette. The non-linear neutral gas flow in the private flux and sub-divertor region is modeled based on the Direct Simulation Monte Carlo (DSMC) method, which takes into account the intermolecular collisions as well as the interaction of the molecules with the stationary walls. For this specific configuration, three different pumping port locations, namely in the low and high field bottom sides of the sub-divertor and directly under the dome haven been chosen. It is shown that the optimum pumping port location is found to be directly under the dome, since the pumped particle flux is increased by a factor 2–3 compared to the one, where the port is located inside the low and high field side divertor "shoulders", respectively. In addition, the divertor dome physically restricts the conductance between the private flux region and the main chamber, enabling the compression of the neutral gas. However, the dome has no direct influence on the macroscopic parameters as the number density and the temperature at the pumping port. Furthermore, it is shown that without the dome, a strong outflux of neutrals towards the plasma core and through the x-point and its vicinity can be expected. This outflux can be reduced by a factor of 2 by positioning the pumping port directly under the dome. Finally it is noted that in all the obtained calculations, the flow field remains homogeneous without the presence of vortices. This can be explained by the fact that the studied geometry does not include any high curvature surfaces, which promote the formation of such flow structures.

1. Introduction

The design space of the DEMO divertor cassette from the pumping efficiency point of view requires an assessment, which has to be based on a fundamental investigation considering several geometrical parameters as the position of the pumping port as well as the presence of the dome. The ultimate aim is to address an optimum divertor design in terms of its pumping capability, using the particle transport physics as the main driver. To the best of our knowledge, such an investigation is performed for the first time.

The primary function of the dome is to achieve a high compression of neutrals in the private flux region (PFR) in order to increase the overall pumping efficiency, which is defined as the ratio of the pumped over the incoming neutral particle flux from the divertor vicinity. Additionally, the dome could reduce the neutral reflux to the plasma core through the x-point and shield the pump duct from neutrons. On the other hand, it shadows the bottom surface of the divertor cassette from neutrons and consequently increases the complexity of the divertor design and the corresponding divertor cost.

Furthermore, since the neutral density in the DEMO PFR is expected to be equal to or higher than that in ITER, the corresponding gas collisionality increases and therefore a nonlinear (i.e. collisional) neutral particle transport treatment is required.

In the present work an efficient numerical tool, which is based on the Direct Simulation Monte Carlo (DSMC) method [1,2] has been applied. The DSMC method consists of a stochastic approach, which reproduces the solution of the Boltzmann equation [1]. Just recently, for benchmark purposes, the DSMC algorithm was implemented to model the neutral gas flow in the JET sub-divertor and a successful comparison between corresponding numerical and experimental results has been performed [3,4]. Consequently, the DSMC method is proven to be a reliable numerical tool, on which the design and the optimization of the DEMO particle exhaust could be based.

* Corresponding author.
E-mail address: stylianos.varoutis@kit.edu (S. Varoutis).

http://dx.doi.org/10.1016/j.nme.2017.04.001

Please cite this article as: S. Varoutis et al., Optimization of pumping efficiency and divertor operation in DEMO, Nuclear Materials and Energy (2017), http://dx.doi.org/10.1016/j.nme.2017.04.001

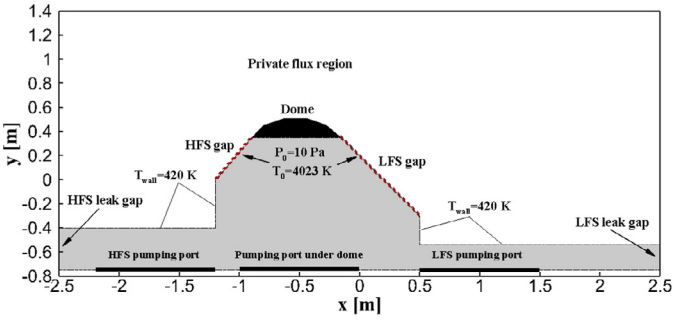

Fig. 1. A 2D axisymmetric geometrical configuration of a simplified divertor design and the corresponding boundary conditions are shown. The pumping surface at the three different locations is indicated as a black solid line. (For interpretation of the references to color in this figure legend, the reader is referred to the web version of this article.)

First simulations, which highlight the influence of the dome structure on the pumping efficiency, have been performed for the ITER divertor [5–8], where it was observed that the dome creates a neutral gas compression independent of the gas species, which is beneficial for the particle exhaust. Furthermore, without the dome an undesirable strong neutral influx towards the plasma core occurs. All the results presented in [5–8] are based on the SOLPS code, which includes the EIRENE algorithm [9], a 3D Monte-Carlo solver for neutral-neutral interactions, based on the BGK kinetic model [10]. It is noted that the main drawback of the BGK model is the inability to correctly describe simultaneously the transport coefficients for gas viscosity and the thermal conductivity. Therefore, the BGK model is commonly applied for the case of pressure driven isothermal flows. Whereas, for the DEMO sub-divertor region with non-isothermal gas flows, we recommend to use the DSMC method.

First assessments of the dome effect in DEMO design have been performed by implementing linear [11] and non-linear [12] particle transport approaches in an ITER-like DEMO divertor configuration. There, it was presented that the dome structure can facilitate the pumping efficiency (about 2 times) and protect the x-point from a strong neutral reflux. In addition, strong asymmetric flow patterns (i.e. vortices) in the divertor plenum were observed, which mainly intercept the path of neutrals towards the pumping port. Those flow asymmetries are typical in viscous flow regime (i.e. high collisionality) and until now no further investigations have been performed on how these asymmetries influence the divertor pumping efficiency. Therefore, the aim of this work is to perform a parametric analysis on a standard divertor configuration, which takes into account the influence of the dome structure and the pumping port location on the whole flow field, including the corresponding macroscopic quantities in the divertor plenum. This analysis will allow defining the design space and the impact of each geometrical parameter on the overall pumping efficiency of the DEMO divertor, which is still under an ongoing conceptual design phase [13].

2. Divertor geometry

A simplified standard divertor configuration is considered in the present work. The PFR below the dome is separated from the plasma fan in the divertor vicinity by two main inclined gaps (highlighted in red dashed lines in Fig. 1) in the high field side (HFS) and low field side (LFS). It is assumed that through these gaps, with poloidal length 0.46 m and 0.92 m (the length of the LFS gap is twice the length of the HFS gap) respectively, only neutral particles penetrate and move towards the sub-divertor volume (shaded area in Fig. 1). In this particular design, the “shoulders”, which end up to the HFS and LFS leak gaps, represent the volume between the divertor cassettes and the vertical divertor targets. The corresponding lengths in the poloidal direction for the HFS and LFS leak gaps are 0.35 m and 0.21 m, respectively. For clarity purposes, it is noted that when a molecule intersects the HFS and LFS leak gaps, it is immediately removed from the computational domain. The poloidal length of the dome structure is equal to 0.75 m. Three representative positions of the pumping surface location have been chosen, namely the pumping surface is located in the entrance of the LFS and HFS divertor “shoulders” and directly under the dome (highlighted as solid black lines in Fig. 1). The poloidal length of all the pumping ports is kept constant and is equal to 1.0 m. Although this problem is in principle of 3D nature, the presented numerical results were calculated for a 2D axisymmetric cut in the toroidal direction.

3. Boundary conditions

Pure molecular deuterium (D_2) gas enters the sub-divertor area through the two HFS and LFS gaps with reference pressure P_0 and temperature T_0 equal to 10 Pa and 4023 K (or 0.35 eV) respectively (see Fig. 1). The applied boundary conditions of pressure and temperature for molecular deuterium correspond to an ITER relevant detached plasma scenario as described in [14,15]. It is noted that in the present work the ionization, dissociation and recombination processes on the walls or in the gas phase are not taken into account. Therefore, when a deuterium molecule hits a stationary wall, it remains as molecule and a purely diffuse reflection takes place, where the incident molecule is reemitted with Maxwellian distribution based on the wall temperature, equal to $T_{wall} = 420$ K (as shown in Fig. 1). The wall temperature is assumed to be uniform along the wall boundaries. In the case of a particle intersecting with the pumping surface, it can be completely removed from the computational domain according to a given probability, which is called capture coefficient ξ. Consequently, ξ takes values between $0 \leq \xi \leq 1$. It is noted that ξ represents the imposed condition of fixed pumped particle flux and is related with the effective pumping speed of the pumping surface [12]. In the present work the capture coefficient takes the following values, namely $\xi = 0.1,\ 0.3,\ 0.6,\ 1$. If the particle is not finally absorbed from the pumping surface, then the particle undergoes a diffuse reflection, assuming that the temperature at the entrance to the pumping port is equal to 420 K. Additionally, when a particle crosses the LFS and HFS leak gaps then, an expansion into vacuum is considered resulting in the complete particle removal. When a particle hits the dome structure then in the case of having a dome, it is reflected diffusely, while in the case without a dome the particle is deleted from the flow domain. The latter assumption can be justified, since an interaction with the plasma takes place and results in the immediate neutral particle ionisation.

4. Numerical modeling

The DSMC method consists of a reliable and powerful numerical tool for modeling rarefied gas flows. According to this method, a gas flow domain is divided into a network of cells. Initial positions and velocities of a large number of model particles are adopted. Each model particle in the simulation represents a large number of real molecules in the physical system. The motion of particles and their collisions are uncoupled by the repetition of the following steps:

- Free motion of particles is modeled, i.e. their new coordinates $\mathbf{r}_{i,\,new}$ are estimated via the old ones $\mathbf{r}_{i,\,old}$ as

$$\mathbf{r}_{i,new} = \mathbf{r}_{i,old} + \mathbf{v}_i \Delta t. \quad (1)$$

Please cite this article as: S. Varoutis et al., Optimization of pumping efficiency and divertor operation in DEMO, Nuclear Materials and Energy (2017), http://dx.doi.org/10.1016/j.nme.2017.04.001

If a particle during the motion crosses a solid surface, then the purely diffuse gas–surface interaction is applied and the particle continues its motion with a new velocity during the rest of time interval Δt.

- Intermolecular collisions are simulated following the Non-Time Counter scheme [1], i.e. the number of pairs to be tested in each cell is calculated as

$$N_{coll} = \frac{1}{2} N_p \bar{N}_p F_N (\sigma_T v_r)_{max} \frac{\Delta t}{V_c}, \quad (2)$$

where N_p is the number of particles in a cell at that moment, $\bar{N}_p$ is the average number of particles in the same cell during all previous steps, F_N is the number of real particles represented by one model particle, σ_T is the total collisions cross-section of the particle, $v_{r,\,max}$ is the maximum relative velocity, and V_C is the cell volume. Two particles from the same cell are randomly chosen and they are accepted for collision under the condition $\frac{\sigma_T v_r}{(\sigma_T v_r)_{max}} > R_f$, where v_r is the relative velocity of this pair and R_f is a random number uniformly distributed over the interval (0,1). If the pair is accepted, their velocities are replaced by new values according to the variable hard sphere (VHS) interaction law [1]. In the VHS model the total cross section is a function of the relative velocity between two collided particles and the viscosity is proportional to T^{ω}, where the parameter ω is called viscosity index and characterizes a given gas. In the present work the viscosity index for molecular deuterium was taken as $\omega = 0.70$. It is noted that after each particle collision the momentum and energy conservation is satisfied.

- Sampling of the macroscopic properties is conducted, i.e. the macroscopic quantities are calculated. The number density n, the bulk velocity vector **u** and the temperature T in a computational cell are estimated respectively through the expressions

$$n = \frac{N_p}{V_C} F_N, \quad \mathbf{u} = \frac{1}{N_p} \sum_{i=1}^{N_p} v_i, \quad T = \frac{m}{3} \left[\frac{1}{N_p} \sum_{i=1}^{N_p} v_i^2 - \mathbf{u}^2 \right]. \quad (3)$$

In all the present simulations an optimum value of $\Delta t = 0.1$ μs has been used, which takes into account the fundamental criterion of DSMC that Δt should be a fraction of the mean collision time τ_{coll}, which is equal to $\tau_{coll} = 13.2$ μs. On the other hand, the average number of particles in each cell of the flow field ranges around 120 particles per cell. This number assures that the statistical scattering of macroscopic quantities along the computational domain is sufficiently low. A structured rectangular grid is applied, with 2.5×10^5 cells. The applied grid was chosen such that the cell size is much smaller than the local mean free path of D_2.

5. Results and discussion

5.1. Flow field

The complete flow field of the collisional molecular deuterium gas flow in the PFR and sub-divertor area has been studied. The main parameters, which describe each flow case, are the location of the pumping port, the capture coefficient ξ and the existence of the dome structure. For the latter, the two extreme cases with and without dome were investigated, the shape of the dome was not changed. For all cases, the incoming boundary conditions were kept constant.

In Fig. 2, the streamlines for the case, where $\xi = 0.3$, the pumping port is located under the dome and without and with dome, respectively, are presented. It is seen that the absence of dome results as expected in an outflux of neutrals towards the x-point. Such a behavior has been observed as well in our previous work [12], where the ITER-like DEMO divertor was studied. Furthermore,

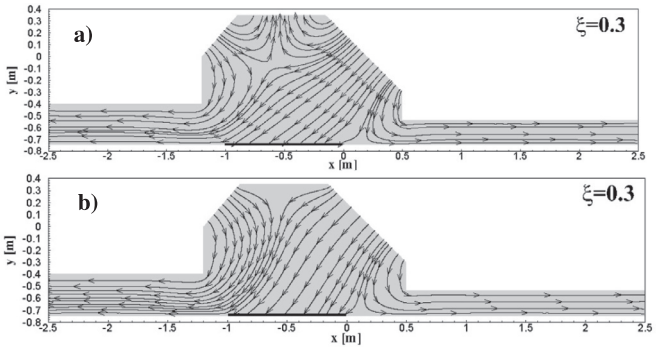

Fig. 2. Streamlines of D_2 inside the sub-divertor plenum for the case of pumping port under the dome, $\xi = 0.3$ and (a) without dome and (b) with dome. The pumping port is indicated as a black solid line..

the pumping port is located within the line of sight of the incoming molecules especially for those entering the LFS gap, and therefore they are much likely to be captured by the pumping surface. The rest of the incoming particles are moving towards and through the LFS and HFS divertor "shoulders", without being influenced by the pumping process.

In the case, where the dome structure exists, the formation of an outflux is eliminated as expected and the neutrals are forced to move towards the pumping port, according to the local temperature and number density gradients. It has been observed that by fixing the pumping port location and by altering the capture coefficient ξ, qualitatively the corresponding flow pattern with or without the dome remains unchanged, while quantitatively all the macroscopic quantities are reduced as ξ increases. These results are not shown here.

In the case of the pumping port being located on LFS or HFS position and without and with dome respectively, it is observed that by shifting the pumping port location in the case with dome, the flow pattern qualitatively remains almost uninfluenced, while in the case without the dome the formation of the outflux still exists.

It is noted that, in all calculated cases, no vortices where observed in the sub-divertor volume as the ones which appeared in [12]. The main reason is that the current configuration still preserves a degree of symmetry, in comparison with the ITER-like DEMO configuration, which consists of several high curvature surfaces that influence the final flow behavior. This is an important result which illustrates the potentially high impact of the geometry on divertor particle exhaust performance.

5.2. Particle fluxes

Assuming that the incoming deuterium gas follows a Maxwellian distribution function, the particle fluxes per toroidal length, which are imposed on the HFS and LFS gaps are equal to $\Gamma_{HFS} = 9.55 \times 10^{16}\,m^{-1}s^{-1}$ and $\Gamma_{LFS} = 1.91 \times 10^{17}\,m^{-1}s^{-1}$ respectively. For convenience purposes, all the calculated and presented particle fluxes are normalized with the total incoming particle flux, which is equal to $\Gamma_{in} = 2.86 \times 10^{17}\,m^{-1}s^{-1}$.

In Fig. 3a, the normalized particle outflux towards the x-point is presented, in terms of the capture coefficient ξ and the different pumping port locations. It is seen that when the pumping port is located on the LFS and HFS divertor "shoulders", the outflux remains unchanged for any value of ξ. The only position of the pumping port, which results in a maximum outflux decrease by a factor of 2, is the position under the dome. In Fig. 3b, the normalized pumped particle flux is presented in terms of capture coefficient ξ and again for various pumping port locations. Here

Please cite this article as: S. Varoutis et al., Optimization of pumping efficiency and divertor operation in DEMO, Nuclear Materials and Energy (2017), http://dx.doi.org/10.1016/j.nme.2017.04.001

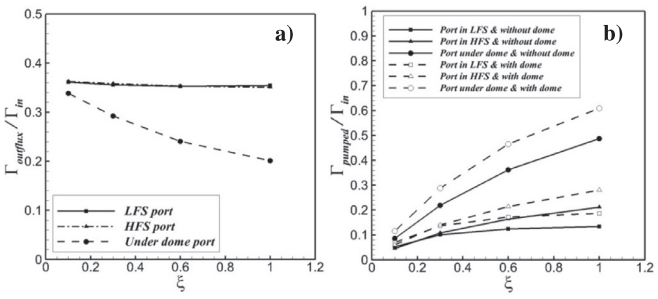

Fig. 3. (a) Normalized particle outflux and (b) normalized pumped particle flux versus the capture coefficient ξ and for various pumping port locations.

it is shown, that qualitatively as ξ increases the pumped flux increases as well until reaching a plateau for all pumping port locations and dome configurations. In addition, by removing the dome structure, a decrease by factor 1.3 in the pumped flux is observed for any ξ and port location. On the other hand, if ξ and the dome configuration remain fixed, while the pumping port location varies, it is deduced that the optimum location which provides the highest pumped flux, is the position under the dome; this finding is in line with the main conclusion drawn from Fig. 3a. When the port is shifted on the HFS and LFS divertor "shoulders" then the pumped flux is reduced by a factor of 2 and 1.5–3, respectively.

5.3. Macroscopic quantities

In this section, the influence of the pumping port location, the capture coefficient and the dome existence on the macroscopic quantities of the local number density and temperature is studied.

As discussed in Section 3, the imposed boundary conditions correspond to a case where high collisionality in the sub-divertor area is expected. Indeed, based on the given pressure P_0 and temperature T_0, the corresponding reference Knudsen number is deduced to be equal to $Kn_0 = \lambda_0/L \approx 0.01$, which corresponds to a highly collisional flow regime. As a characteristic length L of the flow, the square root of the sub-divertor area A (i.e. grey highlighted area in Fig. 1) was chosen, namely $L = \sqrt{A}$, with $A = 2.48\,m^2$. In Fig. 4a, the inverse Knudsen number along the dome height for the case of with and without dome, the pumping port is located under the dome and $\xi = 0.1$ and 1, is highlighted. It is seen that the inverse Knudsen number has high values and as ξ increases, the Knudsen number in the sub-divertor area increases, but still remains at similar collisionality. This behaviour has been observed for all the studied dome configurations and pumping port locations.

In Fig. 4b, the number density distribution along the divertor height is presented for the case of pumping port directly under the dome. It is seen that in the case with dome and $\xi = 0.1$, the number density at $y \approx 0.3$ is increased by a factor of 20, while close to the pumping port at $y \approx -0.7$, is slightly increased by a factor of 1.3, compared with the ones without the dome. Inside the divertor volume, i.e $0.3 < y < -0.7$, an increase of number density by factor of 2 is achieved due to the existence of the dome. By increasing the capture coefficient to $\xi = 1$ (i.e. increase of the pumping speed), then the number density increase at the same above limit positions is of the order of 10 and 1.5 respectively, while in the bulk of the divertor plenum the increase is of the order of 1.5.

As a result, the existence of dome structure results in an increase in the number density in the divertor vicinity, which positively influences the pumping conditions. Additionally, by fixing the dome structure and the pumping port location, the influence of ξ on the number density close to the pumping port is very weak. In Fig. 4c, the temperature distribution is depicted, where the existence of dome results in a cooling of neutrals at $y \approx 0.3$, while the temperature close to the pumping port at $y \approx -0.7$ remains almost uninfluenced. For the area $0.3 < y < -0.7$, a general temperature decrease is observed for any dome and pumping port configuration.

It is noted that the same qualitative behaviour of the flow field is observed when the pumping ports are located in the LFS and HFS "shoulders", while quantitatively the dome structure has a weak influence on the macroscopic quantities.

In Figs. 5 and 6, the contour plots for the number density are presented, for the case of $\xi = 0.3$ and two locations of the pumping port, namely directly under the dome (Fig. 5a) and in the entrance of the LFS divertor "shoulder" (Fig. 5b), and without or with the dome, respectively. In Fig. 5 it is illustrated that by shifting the pumping port directly under the dome a number density drop occurs in the divertor plenum. By introducing the dome structure, in Fig. 6, the number density in the divertor plenum increases and by moving the pumping port directly under the dome, the number density in the main sub-divertor region still is shown to be lower than in the case, where the port is located in the LFS "shoulder". The number density contours are not influenced by the variation of ξ and remain qualitative unaltered. Therefore only the case for $\xi = 0.3$ is shown here.

In conjunction with number density contours, the temperature contours, shown in Fig. 7, seem to remain almost independent on changing the pumping port position and for both dome configurations. Therefore only the cases where the pumping port is located under the dome are depicted. In the case without dome, a zone of hot neutrals occupies almost half of the divertor plenum and by moving downwards to the pumping port a gradual temperature decrease is observed. As long as the particles are flowing through the divertor "shoulders", they are completely thermalized based on the local wall temperature. Furthermore, when the dome is considered, in Fig. 7b, then a clear thermalization of hot neutrals takes place in the dome vicinity and therefore a decrease of the temperature occurs. As for the other predictions, the positions of the pumping port as well as the capture coefficient have a weak effect on the temperature field.

6. Conclusions

In this work, a parametric analysis by using the non-linear DSMC algorithm is performed in order to highlight the influence of the pumping port location and the existence of the dome on the developed flow field and on the overall pumping efficiency of a divertor. For this fundamental study, a simplified divertor geometry is chosen, in which D_2 neutral particles are assumed to penetrate from the LFS and HFS divertor gaps. The chosen incoming boundary conditions correspond to a high-collisionality case, with a Knudsen number of the order of 10^{-2}. These calculations confirm that the position of the pumping port plays a significant role for the pumping efficiency of the divertor and, in particular, the position directly under the dome appears to provide the highest particle removal rate in conjunction with the given positions of the LFS and HFS divertor "shoulders". The port is located in the line of sight of incoming particles and the probability to be pumped is increased. The corresponding pumped particle flux in this case increases by a factor of 2–3 compared to the ones, where the port is located in the LFS and HFS respectively. Furthermore, the divertor dome physically restricts the conductance between the PFR and the main chamber, enabling the compression of the neutral gas. However, the dome has no direct influence on the macroscopic parameters as the number density and temperature at the pumping port. Additionally, it is shown that without the dome, a strong outflux of neutrals towards the plasma core and through the x-point

Please cite this article as: S. Varoutis et al., Optimization of pumping efficiency and divertor operation in DEMO, Nuclear Materials and Energy (2017), http://dx.doi.org/10.1016/j.nme.2017.04.001

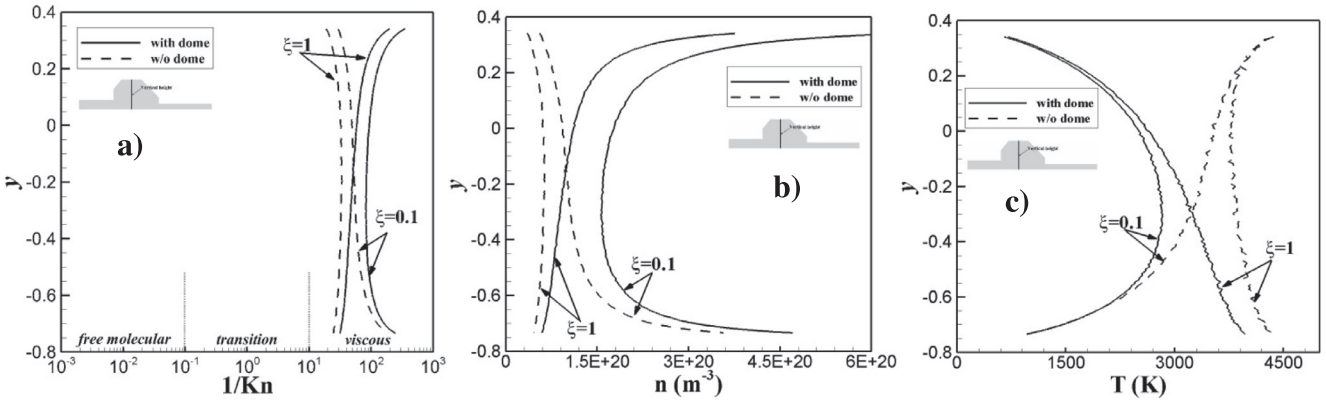

Fig. 4. (a) Knudsen number, (b) number density and (c) temperature distributions along the dome height with and without the dome. The pumping port is located directly under the dome and $\xi = 0.1$ and 1.

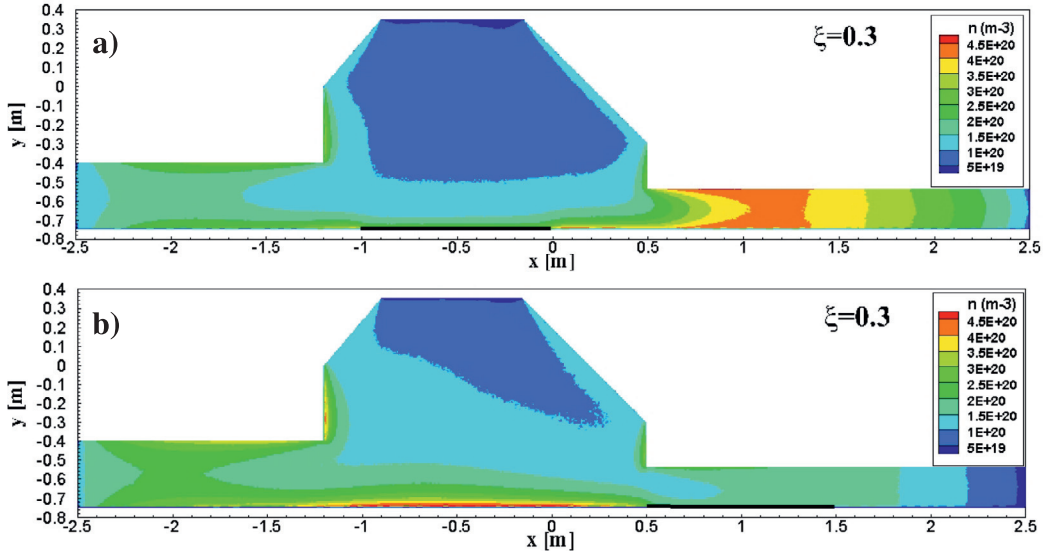

Fig. 5. The number density contours for the case without dome with the pumping port (a) under the dome and (b) in LFS. The capture coefficient is $\xi = 0.3$. The pumping port is indicated as a black solid line.

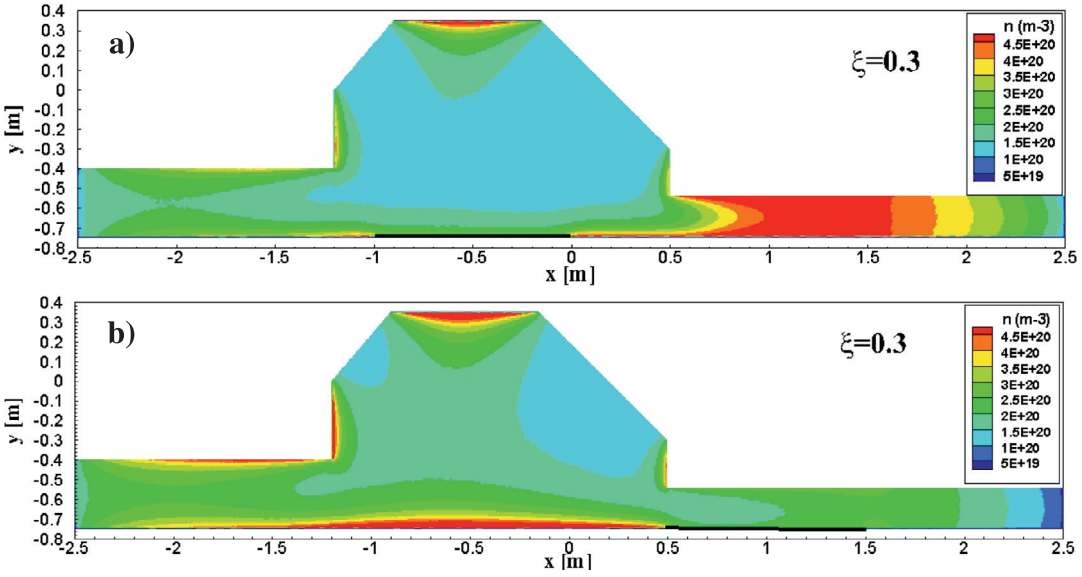

Fig. 6. The number density contours for the case with dome with the pumping port (a) under the dome and (b) in LFS. The capture coefficient is $\xi = 0.3$. The pumping port is indicated as a black solid line.

Please cite this article as: S. Varoutis et al., Optimization of pumping efficiency and divertor operation in DEMO, Nuclear Materials and Energy (2017), http://dx.doi.org/10.1016/j.nme.2017.04.001

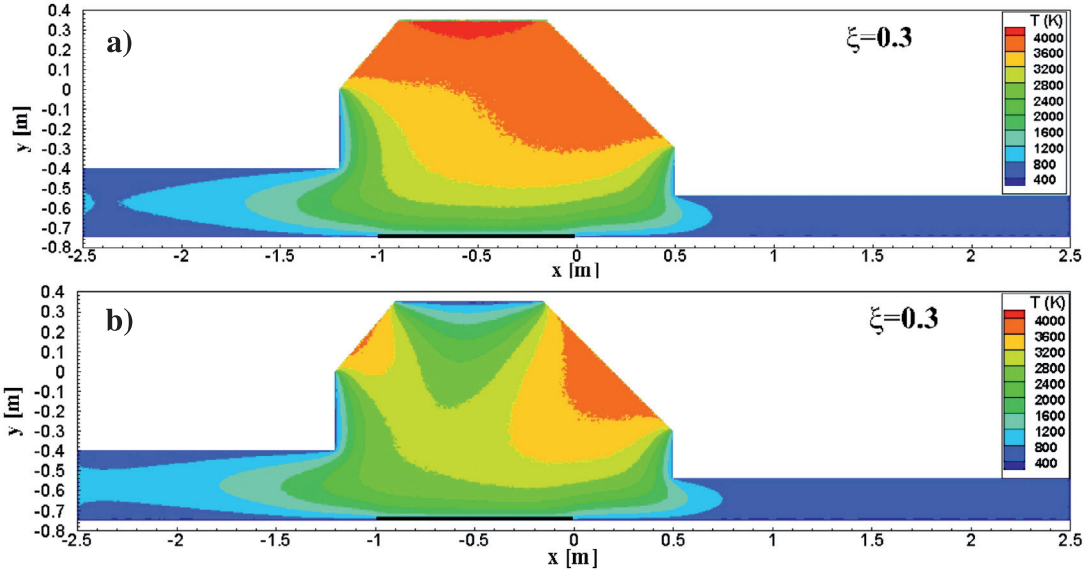

Fig. 7. The temperature contours for the case (a) without and (b) with dome, the pumping port is under the dome and $\xi = 0.3$. The pumping port is indicated as a black solid line.

and its vicinity can be expected. This outflux can be reduced by a factor of 2 by shifting the pumping port directly under the dome. Therefore, the dome structure in the DEMO divertor can be favorable in protection of the x-point region from neutral reflux with consequentially possible thermal instability (MARFE) onset and, eventually, disruption occurrence. Finally it is noted that in all the obtained calculations, the flow field remains homogeneous without the presence of vortices. This can be justified by the fact that the present geometry does not include any surface with high curvature, which promotes the formation of such flow structures.

With regard to DEMO, it has to be noted that the divertor design will have to reconcile also other requirements than those for particle exhaust as discussed in this paper. It is obvious that placing the pumping port directly under the dome has also implications on manufacturability, accessibility, neutron streaming or the potential exploitation of a breeding function in this area. The final design will hence be decided during value engineering later in the DEMO project, when the trade-offs between various options can be better evaluated.

Acknowledgment

This work has been carried out within the framework of the EUROfusion Consortium and has received funding from the Euratom research and training programme 2014–2018 under grant agreement no 633053. The views and opinions expressed herein do not necessarily reflect those of the European Commission.

This work was supported partly by the Broader Approach Agreement between the European Atomic Energy Community and the Government of Japan, which provided resources for the Helios Supercomputer at IFERC–CSC under the Project DSMC–KIT. The rest of this work was performed on the computational resource bwUniCluster funded by the Ministry of Science, Research and Arts and the Universities of the State of Baden-Württemberg, Germany, within the framework program bwHPC.

The authors would like to thank Dr. Michael Gallis from Sandia National Laboratories, USA, for the valuable discussions on the set-up of the Direct Simulation Monte Carlo model.

References

[1] G.A. Bird, Molecular Gas Dynamics and the Direct Simulation of Gas Flows, Oxford University Press, Oxford, UK, 1994.
[2] M. Gallis, et al., Direct simulation Monte Carlo: the quest for speed, in: AIP Conf. Proc., vol. 1628, 2014.
[3] M. Groth, et al., Impact of carbon and tungsten as divertor materials on the scrape-off layer conditions in JET, Nucl. Fusion vol. 53 (2013) 093016.
[4] S. Varoutis, et al., Simulation of neutral gas flow in the JET sub-divertor and comparison with experimental results, in: Proc. of the 25th IAEA Fusion Energy Conference, St. Petersburg, Russia, 2014.
[5] A.S. Kukushkin, H.D. Pacher, V. Kotov, D. Reiter, D. Coster, G.W. Pacher, Improved modelling of neutrals and consequences for the divertor performance in ITER, in: Proc. of the 32nd EPS Conference, Tarragona, Spain, 2005 available online: http://epsppd.epfl.ch/Tarragona/pdf/P1_025.pdf.
[6] A.S. Kukushkin, H.D. Pacher, V. Kotov, D. Reiter, D. Coster, G.W. Pacher, H.P. Zehrfeld, Optimization of the shape of the ITER divertor dome, in: Proc. of the 34th EPS Conference, Warsaw, Poland,, 2007 available online: http://epsppd.epfl.ch/Warsaw/pdf/P1_061.pdf.
[7] A.S. Kukushkin, H.D. Pacher, V. Kotov, D. Reiter, D. Coster, G.W. Pacher, Effects of the dome on divertor performance in ITER, J. Nucl. Mater. vol. 363-365 (2007) 308–313.
[8] H.D. Pacher, A.S. Kukushkin, G.W. Pacher, G. Janeschitz, Scaling of ITER divertor parameters – interpolation from 2D modelling and extrapolation, J. Nucl. Mater. vol. 313-316 (2003) 657–663.
[9] S. Wiesen, ITC-report, 2006. www.eirene.de/e2deir_report_30jun06.pdf.
[10] P.L. Bhatnagar, E.P. Gross, M. Krook, A model for collision processes in gases. I. small amplitude processes in charged and neutral one-component systems, Phys. Rev. vol. 94 (1954) 511.
[11] Chr. Day, S. Varoutis, Yu. Igitkhanov, Initial studies of the divertor dome effect on pumping efficiency in DEMO, in: Proc. of the SOFE Conference, Austin, TX, USA, 2015.
[12] Chr. Day, S. Varoutis, Yu. Igitkhanov, Effect of the dome on the collisional neutral gas flow in the DEMO divertor, IEEE Trans. Plasma Sci. (2016) (accepted for publication).
[13] R. Wenninger, et al., DEMO exhaust challenges beyond ITER, in: Proc. of the 42nd EPS Conference, Lisbon, Portugal, 2015.
[14] V. Kotov, Numerical Study of the ITER Divertor Plasma with the B2-EIRENE Code Package Phd Thesis, FZ Jülich, Germany, 2007.
[15] A.S. Kukushkin, H.D. Pacher, V. Kotov, D. Reiter, D. Coster, G.W. Pacher, Effect of neutral transport on ITER divertor performanace, Nucl. Fusion. vol. 45 (2005) 608–616.